Electronic Spectroscopy and Photophysics of Si Nanocrystals: Relationship to Bulk *c*-Si and Porous Si

L. E. Brus,* P. F. Szajowski, W. L. Wilson, T. D. Harris, S. Schuppler, and P. H. Citrin

Contribution from AT&T Bell Laboratories, Murray Hill, New Jersey 07974

Received November 7, 1994[⊗]

Abstract: The structural characterization, electronic spectroscopy, and excited-state dynamics of surface-oxidized Si nanocrystals, prepared in a high-temperature aerosol apparatus, are studied to gain insight into the emission mechanism of visible light from these systems. The results are compared with direct-gap CdSe nanocrystals, indirect-gap AgBr nanocrystals, bulk crystalline silicon, and porous silicon thin films. As the size of the Si crystallites decreases to 1−2 nm in diameter, the band gap and luminescence energy correspondingly increase to near 2.0 eV, or 0.9 eV above the bulk 1.1-eV band gap. The absorption and luminescence spectra remain indirect-gap-like with strong transverse optical vibronic origins. The quantum yield increases to about 5% at room temperature, but the unimolecular radiative rate remains quite long, $\sim 10^{-3}-10^{-4}$ s^{-1}. The luminescence properties of Si nanocrystals and porous Si are consistent, in most respects, with simple emission from size-dependent, volume-quantum-confined nanocrystal states. Room-temperature quantum yields increase not because coupling to the radiation field is stronger in confined systems, but because radiationless processes, which dominate bulk Si emission, are significantly weaker in nanocrystalline Si. An analogous series of changes occurs in nanocrystalline AgBr. While previous work on CdSe and CuCl nanocrystals has revealed size regimes for their spectroscopic properties, the Si and AgBr nanocrystal studies are shown here to reveal additional size regimes for their kinetic properties.

Introduction

Direct gap semiconductor nanocrystals, such as CdSe, have been extensively studied.[1-4] The unfilled electronic states in these systems become discrete and shift to higher energy as the crystallite size decreases, in semiquantitative agreement with volume quantum confinement theory. The lowest unoccupied state is strongly electric-dipole allowed for all sizes. Detailed studies of the absorption line shape and luminescence dynamics suggest that hole localization on the crystallite surface occurs after photoexcitation.[5,6]

Indirect gap semiconductors, such as Si and Ge, have optical transitions across the band gap that are dipole forbidden but vibronically allowed under translational symmetry in the bulk. The absence of translational symmetry in nanocrystals can be viewed as a weak symmetry breaking: an electronic dipole forms, and the vibronic luminescence becomes size dependent. Both effects are predicted to increase the radiative rate as the crystallite size decreases.[7-10]

While the luminescence from bulk crystalline silicon (*c*-Si) is normally very weak, comparatively intense emission resembling that from nanocrystalline Si is observed in porous-Si (por-Si) films.[11-13] These films are produced by anodic electrochemical etching of *c*-Si in HF solutions, creating a sponge-like porous layer of interconnected 1−10 nm Si crystallites whose surfaces are passivated with H. The etching process itself, which appears to be self-limiting when the quantum confinement energy of the etching hole prevents entry into the nanometer-sized structures, is a relatively simple and quite remarkable approach for synthesizing nanocrystalline material.[14] Photoluminescence from por-Si ranges between 550 and 900 nm, well beyond the 1060-nm band gap of bulk Si, and is observed at room temperature with a few percent quantum yield. The interior surface area is high, and luminescence can be reversibly quenched at high surface pH and by adsorption of polar molecules.[15,16] The luminescent centers appear to be the Si nanocrystals, but a general consensus on a quantitative mechanism is still lacking.

In this paper we study the visible spectroscopy of Si nanocrystals generated from high-temperature aerosols. Preliminary reports have been published in abbreviated form.[17,18] Our analysis here of excited-state dynamics in Si nanocrystals

[⊗] Abstract published in *Advance ACS Abstracts*, March 1, 1995.

(1) (1) (a) Steigerwald, M. L.; Alivisatos, A. P.; Gibson, J. M.; Harris, T. D.; Kortan, K. R.; Muller, A. J.; Thayer, A. M.; Duncan, T. M.; Douglass, D. C.; Brus, L. E. *J. Am. Chem. Soc.* **1988**, *110*, 3046. (b) Kortan, A. R.; Hull, R.; Opila, R. L.; Bawendi, M. G.; Steigerwald, M. L.; Carroll, P. J.; Brus, L. E. *J. Am. Chem. Soc.* **1990**, *112*, 1327.

(2) Weller, H. *Angew. Chem., Int. Ed. Engl.* **1993**, *105*, 41.

(3) Murray, C. B.; Norris, D. J.; Bawendi, M. G. *J. Am. Chem. Soc.* **1993**, *115*, 8706.

(4) Herron, N.; Calabrese, J. C.; Farneth, W. E.; Wang, Y. *Science* **1993**, *259*, 1426.

(5) (a) Bawendi, M. G.; Wilson, W. L.; Rothberg, L.; Carroll, P. J.; Jedju, T. M.; Steigerwald, M. L.; Brus, L. E. *Phys. Rev. Lett.* **1990**, *65*, 1623. (b) Bawendi, M. G.; Carroll, P. J.; Wilson, W. L.; Brus, L. E. *J. Chem. Phys.* **1992**, *96*, 946.

(6) Colvin, V. L.; Alivisatos, A. P. *J. Chem. Phys.* **1992**, *97*, 730.

(7) Hybertsen, M. S. Phys. Rev. Lett. **1994** *72*, 1514.

(8) Takagahara, T.; Takeda, K. Phys. Rev. **1992** *B46*, 15578.

(9) (a) Proot, J. P.; Delerue, C.; Allan, G. *Appl. Phys. Lett.* **1992**, *61*, 1948. (b) Delerue, C.; Allan, G.; Lannoo, M. *Phys. Rev.* **1993**, *B48*, 11024.

(10) Delly, B.; Steigmeier, E. F. *Phys. Rev.* **1993**, *B47*, 1397.

(11) Canham, L. T. *Appl. Phys. Lett.* **1990**, *57*, 1046.

(12) Koyama, H.; Araki, M.; Yamamoto, Y.; Koshida, N. *Jpn. J. Appl. Phys.* **1991**, *30*, 3606.

(13) Petrova-Koch, V.; Muschik, T.; Kux, A.; Meyer, B. K.; Koch, F.; Lehmann, V. J. *Appl. Phys.* **1992**, *61*, 943.

(14) Lehmann, V.; Gösele, U. *Appl. Phys. Lett.* **1991**, *58*, 856.

(15) Chun, J. K. M.; Bocarsly, A. B.; Cottrell, T. R.; Benzinger, J. B.; Yee, J. C. *J. Am. Chem. Soc.* **1993**, *115*, 3024.

(16) Lauerhaas, J. M.; Credo, G. M.; Heinrich, J. L.; Sailor, M. J. *J. Am. Chem. Soc.* **1992**, *114*, 1911.

(17) Wilson, W. L.; Szajowski, P. F.; Brus, L. E. *Science* **1993**, *262*, 1242.

(18) Brus, L. Luminescence of Silicon Nanocrystals and Porous Silicon. *Jpn. J. Appl Phys.*, Proceedings of the International Meeting on Optical Properties of Nanostructures, Sendai, in press.

0002-7863/95/1517-2915$09.00/0

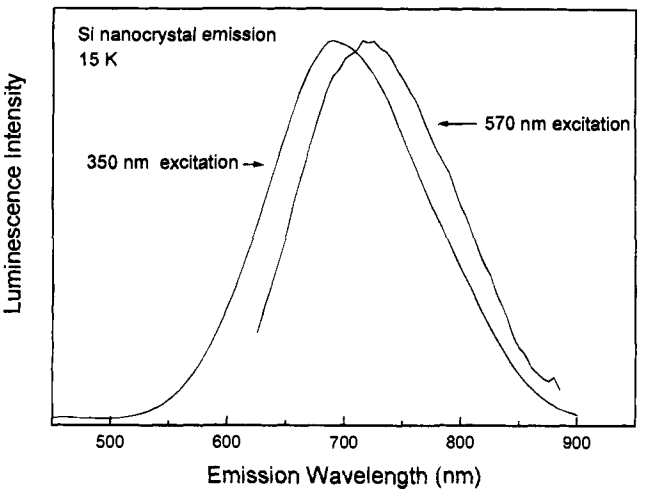

Figure 1. Emission spectra from Si nanocrystals in ethylene glycol glass at ~15 K using 350- and 570-nm exciting radiation.

leads to a deeper understanding of the luminescence from por-Si. In particular, we find that efficient room temperature luminescence occurs in nanocrystalline and por-Si not because of radiative-rate increases in the composite nanostructures, but because of a significant decrease in the radiationless processes of bulk *c*-Si.

Experimental Section

(1) **Synthesis and Structural Characterization.** A two-stage apparatus is used to pyrolyze disilane and make a dilute aerosol of surface-oxidized Si nanocrystals.[19] The aerosol is bubbled through ethylene glycol to create a nanocrystalline colloid. Since there is little size control in the high-temperature process, apart from varying the disilane concentration, the distribution of particle sizes is rather wide. As shown in Figure 1 of ref 17, a narrowed fraction of just small nanocrystals is obtained by size-selective precipitation with tetrahydrofuran.

The luminescence from such a narrowed fraction of nanocrystals, suspended in a frozen ethylene glycol glass at ~15 K and excited by 350-nm light, is shown in Figure 1. It is a structureless Gaussian-shaped band centered at ~700 nm with a fwhm of ~350 meV. The photoluminescence quantum yield of a similar narrowed fraction peaking at ~660 nm is 5.6% at 293 K, which increases to about 50% at temperatures below 50 K.[17] This high quantum yield is obtained following an activation process of heating at 393 K with added acidic hydrogen peroxide. Such activation appears to passivate the last few dangling bonds (interface defect states) in the oxidized nanocrystals.

Larger crystallites, which emit in the 800−1000-nm range, can be seen by bright and dark field transmission electron microscopy (TEM) imaging to be spherically-shaped structures characterized by a 0.5- to 1-nm-thick outer oxide shell encompassing an inner *c*-Si core of >3-nm diameter. As observed by lattice imaging and X-ray powder diffraction patterns, the Si cores are single crystals with lattice constants unchanged from the bulk.[19] Near-edge X-ray absorption spectroscopy (NEXAFS) from these larger crystallites clearly confirms that the particles consist of two main components, *c*-Si and SiO_2, with a minor interfacial sub-oxide component no more than about one monolayer thick.[20]

Structural characterization of the narrowed fraction of smaller nanocrystallites, which emit in the 600−750-nm range, is more challenging. TEM micrographs show these particles to be spherical with outer diameters ≲3 nm, but the internal structure is beyond detection capabilities of either TEM or X-ray diffraction. NEXAFS data, however, reveal that the particles retain the same compositional form, namely, Si, SiO_2, and interfacial SiO_x.[20] From the outer diameters measured by TEM, and the relative amounts of Si in the three components measured by NEXAFS, we find that the nanocrystals luminescing between 600 and 750 nm have Si-core diameters of 0.1−0.2 nm. This corresponds to ~25−200 Si atoms. The outer diameters for the complete series of nanocrystalline particles, varying by a factor of 4, lead to Si-core inner diameters varying by a factor of 7. By contrast, the thicknesses of the outer-SiO_2 and interfacial-SiO_x shells are remarkably similar for all particle sizes, ranging from ~0.6 to 0.8 nm and from ~0.15 to 0.2 nm, respectively. Note that all of these quoted dimensions are average values.

The optical spectra shown below indicate that even the narrowed fraction has red luminescence broadened by the overall size distribution. Accordingly, for these particles it is difficult to give a more precise calibration of luminescence energy versus size.

(2) **Optical Spectroscopy.** Liquid colloids are sealed under air in 2-mm (i.d.) supracil tubes using epoxy. Upon cooling, the liquid ethylene glycol forms a glass with embedded nanocrystals. To obtain excitation spectra over a wide spectroscopic range in an optically thin condition, different concentrations are used and spectra are overlapped. Low resolution (3−4 nm), continuous UV−IR emission and excitation spectra are taken on a double-double calibrated instrument using a W-Xe lamp and a photomultiplier sensitive to 920-nm radiation. Samples are cooled to ~15 K in a flowing He cryostat. Normalized excitation spectra up to 800 nm are obtained by monitoring part of the excitation beam with organic dye solution quantum converters. In a few "photoselection" experiments, a UV polarizer is mounted in the excitation beam, and a Polaroid sheet and quartz scrambler are mounted before the entrance slit of the emission spectrometer. This allows for monitoring of the polarized excitation and emission spectra. In polarization and relative quantum yield experiments, a nonscattering thin frozen sample is obtained by sealing the colloid between sapphire flats separated by a 1-mm-thick Teflon spacer.

Resonant emission is also excited with spectrally narrow, tunable flowing dye or Ti-sapphire lasers between 600 and 800 nm. High-resolution (0.2 nm) spectra are recorded with a CCD camera on a triple spectrometer with gratings blazed for the near-IR. In this apparatus, the sample is immersed in pumped liquid He. The high-resolution data involve time discrimination of several milliseconds, obtained by mechanically chopping the CW laser beam out-of-phase with the luminescence collection beam.

As previously described, lifetime measurement are made using 355-nm, <5-psec excitation at 500 Hz.[17] An analogue transient averager records a photomultiplier signal with ~10 ns time resolution.

Results and Analysis

Figure 1 represents inhomogeneously broadened luminescence: smaller crystallites emit at higher energies while larger crystallites emit at lower energies. Size-selective optical methods—such as luminescence excitation, photoluminescence emission, and transient photophysical hole-burning spectroscopies—have been previously used to obtain single-nanocrystal spectra in studies of direct-gap CuCl and CdSe nanoparticles.[5,21] The resonant hole-burning excitation experiment, which involves detecting a bleaching of optical absorption, would be extremely difficult in por-Si and nanocrystalline Si because the oscillator strength of the band-gap transition is extremely low.

By contrast, the luminescence excitation and emission size selective experiments are feasible because the detection sensitivity of visible luminescence is so high. Monitoring only the high-energy emission at 600 nm while scanning the excitation wavelength provides the optical absorption spectrum from only the smallest nanocrystals. Similarly, scanning the luminescence while exciting the sample near 750 nm provides the emission spectrum from only the largest crystallites.

(19) Littau, K. A.; Szajowski, P. F.; Muller, A. J.; Kortan, R. F.; Brus, L. E. *J. Phys. Chem.* **1993**, *97*, 1224.

(20) Schuppler, S.; Friedman, S. L.; Marcus, M. A.; Adler, D. L.; Xie, Y.-H.; Ross, F. M.; Harris, T. D.; Brown, W. L.; Chabal, Y. J.; Brus, L. E.; Citrin, P. H. *Phys. Rev. Lett.* **1994**, *72*, 2648; *Phys. Rev. B* (to be published).

(21) Itoh, T.; Iwabuchi, Y.; Kirihara, T. *Phys. Status Solidi* **1988**, *B146*, 531.

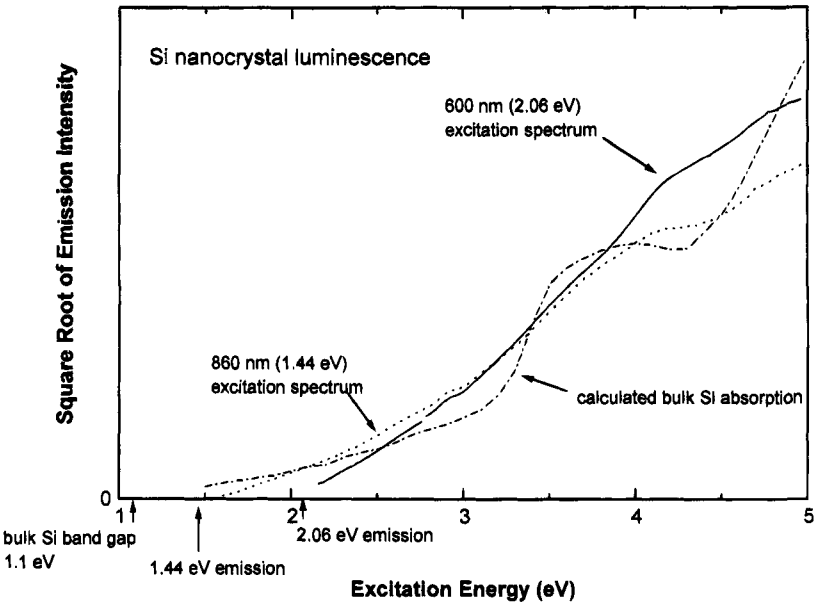

Figure 2. (—) Square root of 600-nm luminescence intensity from Si nanocrystals at ~15 K as a function of exciting radiation energy. (— —) Analogous spectrum for luminescence at 860 nm. Relative normalized intensities of the two excitation spectra have been adjusted so they cross near 3.5 eV. Each trace is a composite of two data sets taken at different concentrations in different spectral ranges. A small bump near 2.9 eV is an artifact of the normalization procedure. (— • —) Square root of the optical absorption cross section of a Si sphere calculated from the electric-dipole term of Mie theory (ref 22) using bulk Si dielectric constants. The calculated curve does not extend below 1.5 eV because bulk Si dielectric data are not available.

(1) Excitation Spectra. Figure 2 shows the excitation spectra at fixed luminescence wavelengths of 600 (2.06 eV) and 860 nm (1.44 eV). The square root of emission intensity is plotted as a function of excitation energy. The spectra, measured from ~0.1 eV above the emission wavelength, monotonically increase in intensity up to 5 eV and cover a dynamic range of 700 for 600-nm emission and 9000 for 860-nm emission. For comparison, the spectrum calculated for *c*-Si (in small particle form) is also displayed.[22]

As opposed to the excitation spectra from CdSe nanocrystallites, which exhibit well-resolved, discrete excited states and more structure than from bulk CdSe,[3] the Si nanocrystallite spectra in Figure 2 are continuous (save a broad feature near 4.2 eV in the 860-nm data) and actually display less structure than bulk Si. The 600-nm spectrum reflects absorption from the smallest crystallites without interference from the larger sizes. It shows approximate straight-line extrapolation back to the emission energy of 2.06 eV. This result implies that (a) in absorption, the nanocrystals exhibit indirect-gap behavior with a band gap of 2.06 eV, and (b) at low resolution, there is no trapping or relaxation between band gap and luminescence. (This latter point is investigated more completely in resonant excitation experiments below.) The 860-nm spectrum shows an apparent band gap about 0.1 eV higher than the emission energy of 1.44 eV, possibly reflecting the wider range of sizes contributing to the comparatively longer wavelength emission.

Bulk *c*-Si excitation spectra are characterized by two distinct regions: indirect-gap absorption from 1.1 to 3.4 eV, and direct-gap absorption from 3.4 to 4.4 eV. Both 600- and 860-nm spectra show an absence of direct-gap absorption. A similar observation has been reported in UV absorption spectra from Si nanocrystals at room temperature.[19] We note that the somewhat well defined 4.2-eV peak in the 860-nm spectrum and the different slopes of the visible and UV absorption data do suggest some evolution toward direct-gap behavior in the UV.

How can these observed differences with CdSe nanocrystallites be understood? In CdSe, two effects contribute to the resolution of discrete structures: (1) the spacings between quantized levels in the *s*-type conduction band are quite large due to the effective mass being only 0.12 m_e, and (2) some transitions are forbidden under dipole selection rules and so are of negligible intensity with respect to allowed transitions. A relatively few, strongly allowed transitions are therefore observed. In Si, the *p*-type conduction band has a significantly larger density of quantized states. Also, the absence of dipole rules in an indirect-gap, vibronically-allowed absorption suggests that all possible transitions will have roughly equal intensity via vibronic coupling. The quantized optical spectrum in Si will therefore be more dense, and in our experiments it will appear continuous. (These transitions may actually overlap with respect to their natural line widths, and thus be truly continuous.)

Why is the 3.4-eV direct-gap region different in nanocrystalline Si than in nanocrystalline CdSe? In CdSe, the quantized conduction-band levels shift monotonically to higher energy with decreasing size because the effective mass is positive in all *k*-space directions. In Si, however, the 3.4-eV transition is a saddle point in *k*-space. This transition in Si might be expected to broaden rather than shift to higher energy, a suggestion worth exploring through quantitative calculation.

(2) Resonant Emission Spectra. If the Si nanocrystalline band-gap transition is vibronically induced, i.e., an indirect-gap transition, then characteristic phonon structures should be present in both absorption and luminescence spectra. In bulk Si, TO (57 meV) and TA (18 meV) vibronic features are observed. In porous Si, resonant emission spectra also show such phonon structure.[23,24]

The low-resolution 570-nm excited emission spectrum in Figure 1 is shifted about 30 nm to lower energy relative to the

(22) Born, M.; Wolf, E. *Principles of Optics*, 3rd ed.; Pergamon: Oxford, 1965; Chapter 13.

(23) Calcott, P. D. J.; Nash, K. J.; Canham, L. T.; Kane, M. J.; Brumhead, D. J. (a) *Phys. Condens. Matter* **1993**, *5*, L91. (b) *J. Lumin.* **1993**, *57*, 257.

(24) (a) Suemoto, T.; Tanaka, K.; Nakajima, A.; Itakura, T. *Phys. Rev. Lett.* **1993**, *70*, 3659. (b) Suemoto, T.; Tanaka, K.; Nakajima, A. *J. Phys. Soc. Jpn.* **1994**, (Suppl. B) *63*, 190.

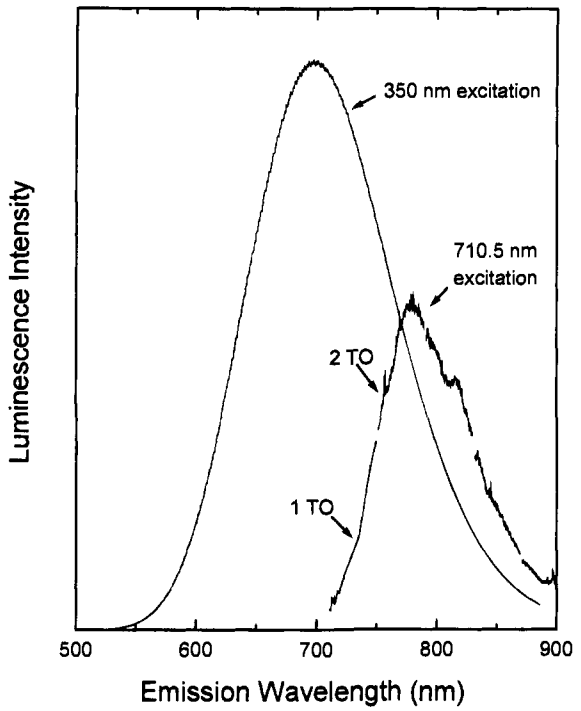

Figure 3. Comparison between the 350-nm excited, low-resolution (3 nm) emission spectrum from Si nanocrystals at ~15 K and the high-resolution (0.2 nm) emission spectrum excited at 710.5 nm. Relative intensities are arbitrary. Weak thresholds, which are Stokes shifted from the 710.5-nm excitation energy, are observed at one and two times the transverse optical (TO) phonon frequency of *c*-Si. Unresolved fine structure in that data, appearing at wavelengths longer than ~760 nm, is shown in finer detail in Figure 7.

350-nm spectrum. A high-resolution 710.5-nm spectrum is shown in Figure 3. It is narrowed, substantially red-shifted with respect to the 350-nm spectrum, and peaked ~150 meV from the exciting laser energy. This is quite different than the resonant emission spectra from CdSe and CuCl, which peak much closer to the laser excitation line.[5,21] The 710.5-nm spectrum also shows two weak thresholds, labeled 1 TO and 2 TO, at energies ~59 and ~112 meV Stokes shifted from the excitation energy.

Analogous red-shifted and narrowed spectra with thresholds have been previously observed in resonance luminescence from por-Si samples. Analysis of those data shows that strong 57-meV structures of 1-TO vibronic origin exist in both absorption and emission.[23,24] The strongest emission is seen in por-Si samples that both absorb and emit resonantly at this vibronic transition, with a Stokes shift of 114 meV from excitation. This is the 2 TO threshold. The weaker 1-TO threshold represents absorption (or emission) on the TO vibronic origin and emission (or absorption) on the weaker zero phonon line (ZPL). There is little emission closer than 57 meV to the excitation.

To gain insight into the spectroscopy of Si nanocrystal luminescence, we model the data generated with 350-, 570-, 660-, and 710.5-nm radiation. For simplicity and lack of better information, the shape of the nanocrystallite vibronic spectrum is assumed to be constant for all particle sizes. We know from Figure 2 that the intensity of the absorption spectrum is continuous and increases nearly quadratically with energy $\gtrsim 0.1$ eV above the nanocrystallite band gap. The higher-energy 350-nm spectrum is therefore more sensitive to the shape of the size distribution and to the intensity of the quadratic absorption relative to vibronic features. The small Stokes-shift regions of the 660- and 710.5-nm spectra are more sensitive to the vibronic spectra near the corresponding nanocrystallite band gaps. The final calculated emission spectrum is taken to be the summed emission from all nanocrystallites whose individual contributions are proportional to their absorption coefficient at the excitation wavelength and to their weight in the size distribution.

Comparison between the calculated and experimental 660- and 710.5-nm emission spectra is given in Figure 4. The size distribution used in obtaining the best common fit to all four resonantly excited spectra is a slightly asymmetric Gaussian, see Figure 5. Note that because absorption increases so strongly with excitation energy (see Figure 2), the 350-nm excitation spectrum more strongly weights the larger crystallites. This explains why in Figure 5 the peak intensity of the size distribution at ~650 nm is energetically higher than the ~700-nm peak emission intensity for excitation at 350 nm.

Figure 6 shows the single-nanocrystal vibronic spectrum used in the fits of the 660- and 710.5-nm emission data. The spectrum has three separate regions, each of which is necessary to fit all the data. The most intense feature is the TO vibronic transition in the 50−100-meV region. Essentially continuous absorption in the 0−50-meV region accounts for about one-third of the integrated intensity of the TO feature. This absorption could represent the ZPL and/or the TA vibronic structure. There is also weak emission in the 100−200-meV region. In order to fit the data, the 0−50-meV feature must be present, but its intensity cannot be significantly stronger than in Figure 6 (i.e., it must be <50% of the TO integrated intensity). Carrier trapping has been suggested for porous Si,[25] which would appear in our model as an additional gap between absorption and emission. However, using a gap as small as 50 meV, for example, clearly produces a worse fit.

The 710.5-nm spectrum is the narrowest and most peaked of the four spectra because it sits on the low-energy, steeply decreasing part of the size distribution. Conversely, the 660-nm spectrum has a flat top because excitation occurs near the peak of the size distribution. Our fits are similar to those reported for por-Si.[23,24] Also, the shape of the spectrum in Figure 6 closely resembles that calculated[7] for nanocrystalline Si (without trapping): both reflect a dominant TO feature with a weaker ZPL and TA absorption.

In Figure 4, note that the spectra are smooth for Stokes shifts less than 2 LO, i.e., <115 meV. For larger Stokes shifts, we observe irregular yet reproducible fine structure, as shown in Figure 7 using higher resolution. Generally speaking, such structure could arise from sharp transitions in relaxed luminescence, or from Raman-like transitions with constant offset from the excitation line. Indeed, a few sharp (0.15-nm wide) lines, particularly the doublet near 755 nm, do behave like Raman lines. The majority of the structure, however, is broader (~0.6 nm) and relatively constant for small changes in excitation wavelength, characteristic of unresolved sharp luminescence.

Our interpretation of the observed fine structure implies that if a Si single nanocrystal was excited and subsequently emitted on the vibronic TO transition, the transition would be sharper than the ~50-meV-wide TO transition depicted in Figure 6. The need for such a wide TO transition is traceable to the size distribution of the Si nanocrystallites. Our model is the simplest one that reproduces the general shape of all spectra, and assumes that all nanocrystals with a given band gap yield identical spectra, ignoring variations of shape, interface structure, etc. These additional distributions effectively widen the vibronic transitions under resonant excitation. It is likely that when more monodisperse/uniform nanocrystals become available, sharper transitions will be observed.

(25) Koch, F.; Petrova-Koch, V.; Muschik, T. *J. Lumin.* **1993**, *57*, 271.

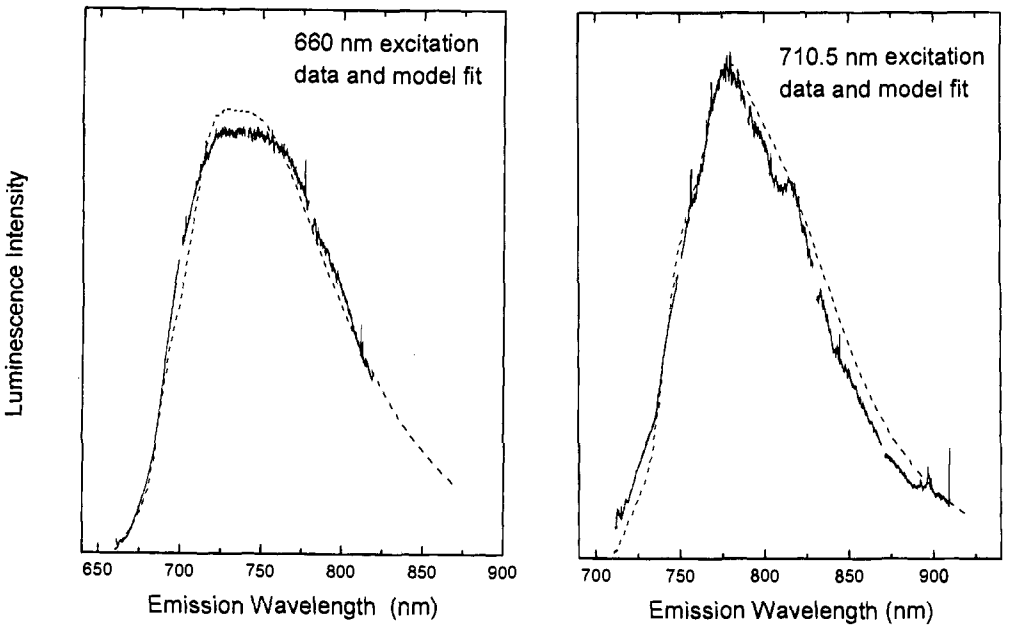

Figure 4. (—) High-resolution emission spectra from Si nanocrystals at ~2 K excited at 710.5- and 660-nm radiation. (The weak structure in the 712–718-nm region of the 710.5-nm spectrum is due to Raman scattering from the cell and ethylene glycol.) (– –) Fits to the data using the model described in the text.

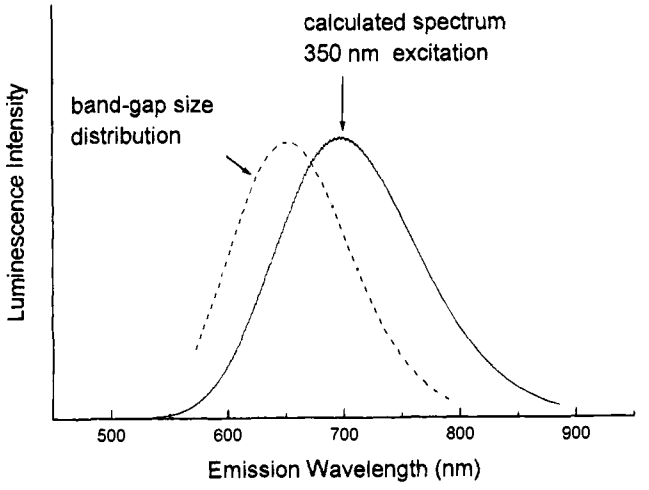

Figure 5. (– –) Mass-weighted band gap (i.e., size) distribution derived in the model fit to 350-, 570-, 660-, and 710.5-nm spectra. (—) Calculated 350-nm luminescence spectrum from the model fit to data shown in Figure 1. Relative intensities are arbitrary.

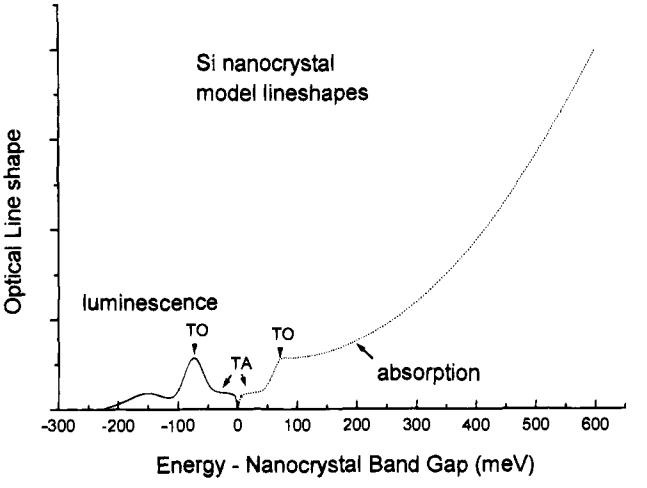

Figure 6. Si single-nanocrystal luminescence (—) and absorption (• • •) spectra derived in the model fit. Negative energies correspond to luminescence below the nanocrystal band gap and positive energies to absorption above the band gap. Transverse optical (TO) and transverse acoustical (TA) vibrations refer to assignments from refs 7, 23, and 24.

(3) Lifetimes and Luminescence Polarization. Luminescence lifetimes as a function of temperature and emission wavelength (630, 730, and 830 nm) appear in Figure 3 of ref 17. The decay is seen from that work to be nearly multiexponential. At 630-nm emission, for example, an average lifetime of 50 μs at 300 K monotonically decreases to about 2.5 ms at 20 K. Luminescence quantum yields have also been measured relative to a known rhodamine dye standard, with corrections for emission spectra and excitation optical density.[17] The room temperature quantum yield is found to be 5.6%, increasing to 50% at temperatures below 50 K.

The extremely long lifetimes allow Raman scattering to be separated from relaxed luminescence. This is accomplished by mechanically chopping the laser beam so that it is blocked when the luminescence is collected. This procedure discriminates against prompt scattering and "early" luminescence during the first millisecond. The LO thresholds and emission spectra are found to be unchanged, confirming that they represent relaxed emission on the time scale of several milliseconds.

In a frozen yet optically clear sample sandwiched between sapphire plates, the degree of polarized luminescence following linearly polarized excitation was measured at 15 K. The ratio $I_{\perp}/I_{\parallel}$ was 1.0 ± 0.05 for excitation wavelengths ≥280 nm, independent of emission wavelength in the range 600–900 nm. Such unpolarized emission implies that the optical absorption and emission dipoles are uncorrelated in direction, as could occur, e.g., in a spherically symmetric system.

Discussion

(1) Quantum Confinement and Comparison with Porous Silicon. The Si nanocrystal spectroscopic and dynamic data are very similar to the data of por-Si. Both show Gaussian-like photoluminescence in the 550–900-nm range, and similar microsecond to millisecond lifetimes as a function of temperature.[11–13,26] Both show indirect-gap-type excitation and size-selective luminescence spectra.[20,23,24] Both show a radia-

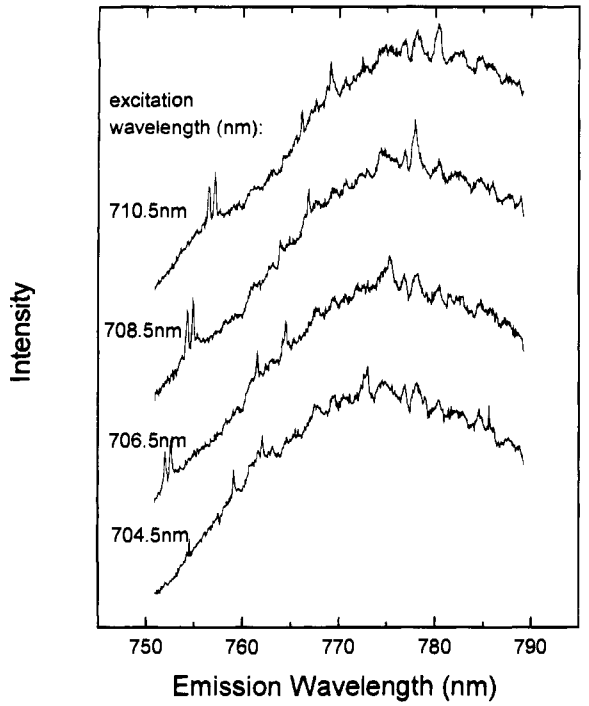

Figure 7. Reproducible fine structure observed in luminescence from Si nanocrystals at ~2 K as a function of excitation wavelength between 704.5 and 710.5 nm. Intensities are arbitrary, and traces have been vertically offset for clarity. The complete 710.5-spectrum is shown in Figure 4.

tionless deactivation around room temperature that can be simply modeled by tunneling through a surface barrier.[17,26] Based on these findings, we conclude that the luminescing chromophore is the same in the two systems.

The data are in semiquantitative agreement with a simple model of nanocrystal quantum confinement in which there is a luminescing $1S_e-1S_h$ band-gap state and no significant "trapping" between the optical absorption band gap. (The 1S notation implies that both electron and hole are in totally symmetric volume-confined states.) The optical spectra evolve with size from the bulk *c*-Si band gap to 650-nm emission for ≤1.5-nm nanocrystals. The size-selective emission spectra show dominant LO phonon structure with weaker TA and ZPL contributions, in agreement with theory.[7] The effective radiative lifetime has a temperature dependence consistent with equilibration between lower-lying millisecond and a higher-lying microsecond levels, as predicted by consideration of the spin- and valley-orbit fine structure of the lowest $(1S_e-1S_h)$-envelope-function state.[9,23]

That these data are observed in nanocrystals with oxide passivation, and in porous Si with hydride termination, indicates it is the presence—not the chemical nature—of the passivated surfaces that is important. This, in turn, suggests that the luminescing wave function is most likely confined not to the passivated atoms but to the inner Si atoms, as occurs in the $1S_e-1S_h$ state. Our conclusion here contrasts with that of Kanemitsu, who assigns the luminescence to interface states.[27]

There appears to be inconsistency between our results and theoretical calculations. In particular, correlations between theoretical band gaps and Si particle sizes[7-10,28] predict ≥2.5-eV band gaps for the ≤1.5-nm crystallites that we find emitting near 650 nm (1.9 eV). This difference might occur if there were "trapping", or some type of structural relaxation between absorption and luminescence. The optical spectra, however, show no sign of a higher band gap. Another possible explanation is that the effective electron-hole (e-h) Coulombic interaction has been underestimated in such small nanocrystallites, and this would decrease the calculated band gap. One treatment of such interactions,[28] however, still shows large discrepancies between theory and experiment in the small particle regime. Very recently, new calculations using a different basis set of unfilled atomic orbitals have been reported,[29] and these yield significantly smaller band gaps than in other work.[7-10,28] Future inclusion of the e-h interaction should lower the effective band gap even further.

Another apparent inconsistency is the effective radiative lifetime of $\Gamma_r = 2 \times 10^3\ s^{-1}$, which we obtain for 650-nm emission. This value is about an order of magnitude longer than that calculated[7] for particles of this size. It is possible that the luminescing state may be distorted in some way. A distorted $1S_e-1S_h$ state would decrease the e-h overlap and increase the radiative lifetime; it would not, however, produce trapping that is detectable at the present resolution. Future, higher-resolution experiments will be needed to reveal evidence for such possible distortion.

While the nanocrystalline Si and por-Si data are similar in many ways, there are differences. The size-selective excitation data of Calcott et al.[23] from their hydride-terminated por-Si samples show sharper TO and TA structure than data from our oxidized Si nanocrystallites or from the hydride-terminated por-Si samples of Suemoto et al.[24] This suggests that the distributions of shape and/or interface roughness occurring for a given band-gap energy are larger in the latter two experiments (interface roughness might distort the emitting wave function). Recall from the NEXAFS data of Si nanocrystallites, however, that the effective interfacial oxide thickness is consistently about one monolayer.

Unlike the polarized luminescence data from our Si nanocrystallites, the luminescence from por-Si following polarized excitation is strongly linearly polarized.[30] Thus, the transition dipole is nondegenerate and has the same orientation in space despite energy relaxation from 350-nm excitation to 700-nm emission. This would occur in elliptically shaped crystallites if the dominant dipole were along the principal axis. Indeed, TEM studies of por-Si often show elliptical structures. The preservation of polarization, in spite of energy relaxation, is important because it implies that the wave function in both absorption and emission reflects the crystallite shape. That is, the wave function is delocalized over the entire nanostructure. (In a bulk semiconductor, all polarization information would be lost following energy relaxation of this magnitude.) In the Si nanocrystallites, such polarization is absent because our aerosol procedure produces nearly spherical particles with spatially degenerate dipoles.

It has been a goal to make por-Si samples that luminesce in the green and blue region, i.e., at 2.5–3.5 eV.[31] Our data suggest that this has not been realized because the "maximum" band gap, corresponding to the smallest nanocrystal size of ~1 nm, is ~2.5 eV. Another way of estimating the limit between

(26) Vial, J. C.; Bsiesy, A.; Gaspard, F.; Herino, R.; Ligeon, M.; Muller, F.; Romenstain, R.; Macfarlane, *R. M. Phys. Rev.* **1992**, *B45*, 1417.
(27) (a) Kanemitsu, Y. *Phys. Rev.* **1993**, *B48*, 12357. (b) Kanemitsu, Y.; Ogawa, T.; Shiraishi, K.; Takeda, K. *Phys. Rev.* **1993**, *B48*, 4883. (c) Kanemitsu, Y. *Phys. Rev.* **1994**, *B49*, 16845.
(28) Wang, L.; Zunger, A. *J. Chem. Phys.* **1994**, *100*, 2394.
(29) Hill, N. A.; Whaley, K. B. *Mater. Res. Soc. Symp. Proc.* To be published.
(30) Andrianov, A. V.; Kovalev, D. I.; Zinovev, N. N.; Yaroshetskii, I. D. *Sov. Phys. JEPT Lett. (Engl. Transl.)* **1993**, *58*, 427.
(31) A blue emission of short lifetime is apparently due to a hydroxyl impurity in silicon dioxide, *cf.*: Tamura, H.; Ruckschloss, M.; Wirschem, T.; Vepreck, S. *Appl. Phys. Lett.* **1994**, *65*, 1537.

Si particle size, band gap, and luminescence energy is to consider a recently synthesized class of octasilacubane molecules, R_8Si_8 (R = trimethylpropyl groups).[32] These molecules, containing somewhat distorted Si−Si bonds at almost 90° angles, can be viewed as models for the smallest possible three-dimensionally bonded Si nanocrystal. The lowest excited state in these indirect-gap molecules lies in the range between 2 and 2.5 eV. At room temperature, ~2.5-eV luminescence of long lifetime is observed.

(2) Comparison with Bulk Crystalline Silicon. The luminescence from a single e-h pair electrically isolated in one Si nanocrystal is essentially molecular emission, describable by competing first-order unimolecular radiative and nonradiative decay rates, Γ_r and Γ_{nr}. In *c*-Si at room temperature, however, an e-h pair is unbound with respect to *kT*. Carriers separate and the "excited state" is describable only in terms of mobile electrons and holes scattering off each other over macroscopic distances. Theoretically, it is difficult to compare these very different luminescence processes, but experimentally, the contrast is clear: At room temperature, Si nanocrystals (as well as por-Si samples) emit with quantum efficiencies of a few percent, while *c*-Si emission is orders of magnitude weaker.

Comparisons can also be made at low temperature, where the e-h binding energy of 14.7 meV in *c*-Si is greater than *kT*.[33] A translationally "free", or shallow trapped exciton in *c*-Si has a diameter of about 3 nm and a measured TO-phonon-induced radiative rate of $\Gamma_r = 2 \times 10^4\ s^{-1}$.[34] Luminescing, distorted excitons in *c*-Si can be trapped at the sites of Be or Ga dopants, for example, where a singlet−triplet fine structure is observed,[35] analogous to the fine structure observed in por-Si.[23] At low temperature, therefore, we see that excitons in *c*-Si and e-h pairs in Si nanocrystals both have long and approximately similar radiative decay rates. In both systems, the electron and hole are confined in space, the *k*-space selection rules due to translational symmetry are not strictly valid, yet the systems remain indirect gap. Note also that at low temperatures both systems are similar in that $\Gamma_{nr} \ll \Gamma_r$, despite the low value of Γ_r. The *c*-Si lattice is rigid, and the exciton−phonon coupling responsible for multiphonon radiationless decay is extremely weak.

At room temperature, the e-h pairs in nanocrystals remain bound and continue to emit at a relatively slow rate. By contrast, the e-h pairs in *c*-Si separate and the individual carriers scatter over macroscopic distances, inviting nonradiative processes to consume the carriers. One such process involves deactivation at defects/deep traps. Even in crystals with relatively low defect densities, the carriers live long enough to find these traps and then recombine nonradiatively.

In near-perfect room-temperature crystals with hydrogen-terminated surfaces, an excess population of free electrons and holes at very low densities, e.g., $\sim 10^{14}\ cm^{-3}$, lives for many milliseconds.[36] At higher densities, efficient nonradiative Auger recombination dominates the kinetics, i.e., e + h + (e or h) → (e or h) + 1.1 eV kinetic energy. (Note that this process is purely electronic and independent of exciton−phonon coupling.) Thus, at normal or even modest illumination intensities, both the nonradiative trap and Auger processes quench the luminescence in *c*-Si.

These two radiationless processes, which are so important in the bulk, are much less significant in the nanocrystals. Auger decay is obviously slower when e-h pairs in separate crystallites cannot interact. Similarly, deep trap deactivation is decreased when a defect can only quench emission from the one crystallite containing it (in bulk Si, of course, a single trap can quench emission from a much larger volume). Thus, if passivating the nanocrystals introduces no new nonradiative processes, luminescence in nanocrystals will increase with respect to bulk *c*-Si. From this discussion we see that room temperature luminescence is more efficient in nanocrystalline Si—and by extension, por-Si—not because coupling to the radiation field is stronger in confined systems, but because the radiationless processes dominant in *c*-Si are much less important.

The observed increase in photoluminescence efficiency is, therefore, simply a consequence of kinetics caused by the barriers to carrier mobility between crystallites. It is these same barriers, of course, which create quantum confinement. Our arguments should apply to any conductive solid with comparatively few traps. Read et al.[37] and Koch et al.[25] have also argued that some of the luminescence enhancement in por-Si is due to reduced carrier mobility to deep traps.

(3) Size Effects in Indirect-Gap Semiconducting AgBr Nanocrystals. AgBr with iodine atom impurities at the 10^{-6} level, used as micron-sized crystals in photography, shows "impurity size exclusion" as nanocrystals.[38,39] Crystallites larger than 10 nm contain iodine atoms and show iodine-trapped exciton emission, while smaller nanocrystals are iodine-atom free and show free excition emission. AgBr also contains unidentified deep nonradiative traps at the 10^{-5} level which quench luminescence. As these traps are reduced, the net luminescence increases with decreasing diameter, *d*, as $d^{-3.6\pm1.2}$, slightly faster than inversely proportional to volume.[39] Direct measurement of the free exciton lifetime (presumably purely radiative) at 6 K shows a decrease from 920 to 350 10^{-6} s for *d* from 12 to 6 nm.[38d] A weak, purely electronic ZPL is present in the luminescence at small sizes. Thus, while the lifetime does shorten slowly in nanocrystals, the material remains essentially indirect-gap-like. Luminescence increases in AgBr nanocrystals because traps are excluded, and because the surface passivation is good, just as in the Si system.

(4) Size Regimes for Semiconductor Nanocrystals. For some time, size regimes in the evolution of semiconductor spectroscopic properties have been understood.[40,41] As shown in Figure 8, these can be labeled with increasing size as molecular, quantum dot, polariton, and finally (not shown) bulk semiconductor species. Broadly speaking, these species represent the evolution of molecular to unit-cell structures, discrete electronic states to continuous bands, and weak dipole scattering to strong macroscopic, polariton electromagnetic scattering.[42]

(32) (a) Matsumoto, H.; Higuchi, K.; Hoshino, Y.; Koike, H.; Naoi, Y.; Nagai, Y. *J. Chem. Soc., Chem. Commun.* **1988**, *1083*. (b) Matsumoto, H.; Higuchi, K.; Kyushin, S.; Goto, M. *Angew. Chem., Int. Ed. Engl.* **1992**, *31*, 1354.

(33) Shaklee, K. L.; Nahory, R. E. *Phys. Rev. Lett.* **1970**, *24*, 942.

(34) (a) Haynes, J. R.; Lax, M.; Flood, W. F. *Proc. Int. Conf. Semicond. Phys.* **1961**, *423*. (b) Cuthbert, J. D. *Phys. Rev.* **197**, *B1*, 1552.

(35) (a) Thewalt, M. L. W.; Waltins, S. P.; Ziemelis, U. O.; Lightowlers, E. C.; Henry, M. O. *Solid State Commun.* **1982**, *44*, 573. (b) Schall, U.; Thonke, K.; Sauer, R. *Phys. Status Solidi* **1986**, *B137*, 305.

(36) Yablonovitch, E.; Allara, D. L.; Chang, C. C.; Gmitter, T.; Bright, T. B. *Phys. Rev. Lett.* **1986**, *57*, 249.

(37) Reed, A. J.; Needls, O. R. J.; Nash, K. J.; Canham, L. T.; Calcott, P. D. J.; and Qteish, A. *Phys. Rev. Lett.* **1992**, *69*, 1232.

(38) (a) Johansson, K. P.; McLendon, G. P.; Marchetti, A. P. *Chem. Phys. Lett.* **1991**, *179*, 321. (b) Johansson, K. P.; Marchetti, A. P.; McLendon, G. P. *J. Phys. Chem.* **1992**, *96*, 2873. (c) Marchetti, A. P.; Johansson, K. P.; McLendon, G. P. *Phys. Rev.* **1993**, *47*, 4268. (d) Chen, W.; McLendon, G.; Marchetti, A.; Rehm, J. M.; Freedhoff, M.; Myers, C. *J. Am. Chem. Soc.* **1994**, *116*, 1585.

(39) Kanzaki, H.; Tadakuma, Y. *Solid State Commun.* **1991**, *80*, 33.

(40) Brus, L. *J. Phys. Chem.* **1986**, *90*, 2555.

(41) Efros, Al. L.; Efros, A. L. *Sov. Phys. Semicond. (Engl. Transl.)* **1982**, *16*, 1209.

(42) For a discussion of this evolution, see: Brus, L. In *Springer Series in Chemical Physics 56: Clusters of Atoms and Molecules II*; Springer-Verlag: Berlin; Haberland, H., Ed.; p 312.

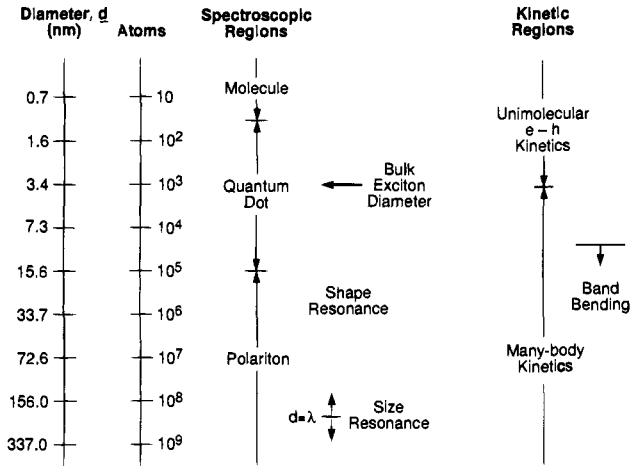

Figure 8. Schematic representation of size regimes used for describing spectroscopic and excited-state kinetic properties of semiconductor nanocrystals.

Experimental examples are provided by extensive studies from direct-gap CdSe and CuCl systems.

The Si and AgBr nanocrystalline data show that the distinction between direct and indirect gap is realized with increasing size much more quickly than the numerical value of the band gap suggests. In Si, where the conduction band minimum traverses almost completely across the Brillouin zone from the valence band maximum at Γ, the electron phase changes almost completely from one unit cell to the next. Thus, intra-unit-cell optical transition dipoles will destructively interfere in nanocrystals made of just several unit cells. By contrast, the band gap evolves slowly in materials such as Si and especially CdSe, which contain small effective masses.[40,41]

The Si and AgBr systems also allow us to recognize the existence of a separate family of size regimes for kinetic properties. In semiconductors with high mobilities, the kinetic pathways and the quantum yields for various processes can be completely changed by "size exclusion" of impurities at the levels of ppm and lower. Furthermore, the importance of processes involving the interaction of several e-h pairs, such as the Auger process, systematically decreases as size decreases because the photoexcitation rate per crystallite generally scales with crystallite volume. Marchetti et al. have also stressed these latter two points in the low-temperature spectroscopy of AgBr nanocrystals.[38c] Finally, in quantum dots at room temperature, e.g., red-emitting Si nanocrystals, the e-h pair is "confined" in terms not typically used for such systems, namely, by kinetic barriers to molecular excited-state decay of a single pair on a single dot.

Acknowledgment. The NEXAFS experiments were performed at the NSLS, Brookhaven National Laboratory, which is supported by the DOE, Division of Materials Science and Division of Chemical Sciences. We thank M. Hybertsen and Y.-H. Xie for valuable discussions.

JA943638H